Polymer 51 (2010) 3660–3668

Contents lists available at ScienceDirect

Polymer

journal homepage: www.elsevier.com/locate/polymer

Enhanced crystallization kinetics in poly(ethylene terephthalate) thin films evidenced by infrared spectroscopy

Monica Bertoldo [a,*], Massimiliano Labardi [b], Cinzia Rotella [c,1], Simone Capaccioli [b,c]

[a] PolyLab-INFM-CNR, Via Risorgimento 35, I-56126 Pisa, Italy
[b] PolyLab-INFM-CNR, Largo Pontecorvo 3, I-56127 Pisa, Italy
[c] Department of Physics, University of Pisa, Largo Pontecorvo 3, I-56127 Pisa, Italy

ARTICLE INFO

Article history:
Received 28 January 2010
Accepted 20 May 2010
Available online 9 June 2010

Keywords:
Poly(ethylene terephthalate)
Crystallization
Ultrathin films

ABSTRACT

The cold crystallization process in poly(ethylene terephthalate) (PET) spin-coated ultrathin films was studied by infrared spectroscopy. The conformational change associated to the formation of crystal phase during annealing at 107 °C was measured in real time, by monitoring both intensity and frequency shift of *trans* and *gauche* conformer bands of the PET glycol segment. Enhancement of crystallization kinetics was observed in thin films deposited on amorphous silicon, with respect to a 20 μm thick free standing film used as reference, where the fastest kinetics was observed for the thinnest (35 nm) film. Experimental findings were interpreted in terms of scarce interaction between PET films and silicon substrate, which does not provide slowing down of crystallization kinetics as observed on different substrates. This results in a dominant effect of the polymer/air interface, where faster kinetics is observed, as also confirmed by atomic force microscopy imaging, particularly on the thinnest film. Additionally, Avrami and Avramov analyses evidence a decrease of both the Avrami exponent, related to growth dimensionality, and induction time, related to delay of nucleation start, when decreasing film thickness. Therefore, the reported results enrich the description of confinement and substrate interaction effects on the cold crystallization process taking place in PET ultrathin films.

1. Introduction

The behavior of polymers in nano-pores, nano-channels, nano-layers as well as polymer nano-particles, nano-rods and nano-films is of wide interest to the scientific and applicative development of soft matter nanotechnologies since all the mentioned geometries are examples of confined spaces. Indeed, properties of polymers such as the glass transition, the melting temperature and the crystallization kinetics may differ in confined geometry in more or less extent from the corresponding properties of the unperturbed materials in the bulk [1].

It is widely accepted that polymer crystallization at surfaces and interfaces differs somehow from bulk crystallization, while the reasons for this behavior are still under debate. Nucleation from impurities concentrated at the exposed surface has been often invoked in the past [2,3], while more recently, phenomena connected to the different dynamics of the polymer at the interface have been considered [4,5].

Among polymers, poly(ethylene terephthalate) (PET) can be chosen as a model material to study crystallization in confined geometry, because its crystallization rate is slow enough to allow isothermal studies also under accelerated conditions such as those that may be found in confined geometries [6]. Moreover, PET is an important material for large scale applications such as packaging films and bottles as well as for electronics, due to its good optical, electrical and gas barrier properties, as well as to its quite high melting temperature. For all the mentioned applications and in particular in view of combining packaging and electronics, the properties of polymers at the interface with air, as well as with those metals that are typically used for electronics, may be of crucial importance.

Several works have dealt in the last years with the behavior of PET in confined geometries [7–10]. In particular, its glass transition temperature in ultrathin films on gold was found to decrease monotonically with the film thickness when the latter is smaller than 100 nm [7]. Crystallization of PET at the air interface studied by AFM, grazing incidence X-ray diffraction and XPS was found in all cases to be faster than the bulk one [11–13].

* Corresponding author. Tel.: +39 (0)502219413; fax: +39 (0)502219320.
E-mail address: monicab@dcci.unipi.it (M. Bertoldo).
[1] Present address: Department of Physics and Astronomy, Leuven University, Celestijnenlaan 200d - bus 02416, B-3001 Leuven, Belgium.

0032-3861/$ – see front matter © 2010 Elsevier Ltd. All rights reserved.
doi:10.1016/j.polymer.2010.05.040

On the contrary, the crystallization rate and the crystalline fraction in films on gold substrates were both found to decrease with the film thickness [9]. Similarly, a slowing down of structural dynamics was observed by dielectric spectroscopy in PET thin films capped between aluminum electrodes [8]. Such effect was related to a reduced mobility layer at the aluminum interface. Reduction of the crystallization kinetics rate in ultrathin films on silicon substrates was also observed for poly(ethylene oxide) [14] and poly (ethyl-vinyl acetate) [15]. Generally, a reduced mobility of polymers near the interface is invoked to explain the lower crystallization rate. Another explanation for the reduced crystallization rate found in thin films is that the spherulites located near the interfaces or surfaces have a lower probability to include polymer volume in the formation of the crystal with respect to what happens in the bulk [16].

Recently Reiter and coworkers [17] showed, by dynamic Monte Carlo simulations, that a more rich scenario would exist: in fact, both decrease and increase of crystallization rate may be observed in ultrathin films, depending on whether there is attraction or neutral repulsion between polymer and substrate. This indicates that, in principle, a crystallization rate increase could be observed for crystallizable polymers on scarcely interacting substrates. Nevertheless, experimental evidences of such a fact are still missing until now.

In order to assess this predicted behavior, a non metallic substrate with potential interest in electronics applications such as silicon was select as scarcely interacting substrate for PET. Therefore, thin and ultrathin films on silicon were prepared by spin-coating. Silicon in amorphous state was selected because it is mostly transparent in the infrared spectral region and it can be used as support for infrared spectroscopy analysis in the conventional transmission mode. The crystallization of PET was then followed isothermally during annealing at 107 °C by infrared spectroscopy which can provide information on the crystallization process as well as on the polymer conformation and possible interaction at the interfaces [7,15]. Morphology of initial and final surfaces was also obtained by AFM to further support our findings.

2. Experimental part

2.1. Materials and sample preparation

PET sheets of 250 μm thickness were purchased from Goodfellow. Molecular weight average and distribution were characterized by Size Exclusion Chromatography (SEC) using $CHCl_3/CH_2Cl_2$/hexafluoroisopropanol 60/30/10 as an eluent at 1 ml/min. The analysis revealed that the used PET has $M_n = 38800$ kg/mol and $M_w/M_n = 1.97$.

Ultrathin films of various thicknesses were prepared by spin-coating chloroform/trifluoroacetic acid solutions of PET on amorphous silicon IR windows (Nicodom, IR Si transmission windows). Before the polymer deposition, the substrates were sonicated successively in acetone, isopropanol and deionized water. Then, they were cleaned by UV/ozone during 15 min.

Film thickness was varied by changing the solution concentration and spin-coating speed. To allow a gradual solvent evaporation, the samples were annealed under vacuum (10^{-4} mbar) for few days at 30 °C, and progressively heated up to 65 °C (just below the bulk glass temperature $T_g = 71$ °C). Then, the samples were kept at such temperature during 6 additional hours to remove possible mechanical stresses induced by the spin-coating. Annealing above the glass transition temperature was avoided since in that case spherulite formation on the surface occurs, as evident by AFM imaging.

The solvent removal was checked by IR spectroscopy analysis, by monitoring the disappearing of the intense O–H and C=O stretching bands at 3200–3500 cm^{-1} and 1750–1800 cm^{-1}. We found that the total removal of the solvent before the annealing at 65 °C was necessary in order to avoid any crystal formation.

After the last annealing procedure, the film thickness was measured by profilometry.

A free-standing film of PET of ~20 μm thickness, used as reference bulk sample, was obtained by compression moulding (Collin 200P) at 250 °C during few min at 50 bar, and then quenching in water.

2.2. Infrared spectroscopy

Fourier transform infrared (FT-IR) spectra in transmission mode were collected with a Perkin Elmer 1770 spectrophotometer. A total of 32 scans with 4 cm^{-1} resolution were collected for ultrathin films over 3–4 min. 8 scans were collected in the case of the free standing film. Background was acquired every 4 scans on clean reference windows. Single films deposited on substrates were analyzed, excepting for the case of 35 nm ultrathin films, where the absorbance of a single film was too low to obtain reliable IR data. Therefore three films were stacked with teflon O-ring spacers (10 μm thickness) between them, in order to increase absorption (Fig. 1). A similar assembly with clean Si windows was used to obtain the corresponding background measurement. In this case 64 scans were accumulated for both sample and background.

A home-made thermostated sample holder was used for the on-line study of cold crystallization kinetics at 107 °C. Temperature was regulated by Lake Shore 331 controller equipped with T thermocouple (contacted to silicon substrate) and Pt100 A-Grade sensor (embedded into the metallic sample holder). Both sensors measured the same temperature within their accuracy, therefore we can exclude the presence of significant gradient across the sample. Infrared spectra were collected as a function of time, while films were kept at 107.0 ± 0.5 °C. Zero of time was fixed when temperature raised to 104–105 °C, in such a way that temperature stabilized to the final 107 °C during the first point of acquisition. During the first hour of annealing, measurements were performed every ~3 min, and in the following period the time interval between consecutive measurements was progressively increased.

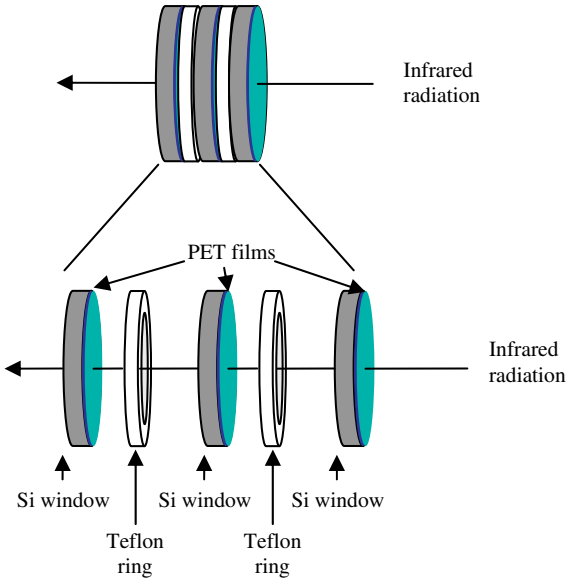

Fig. 1. Stack adopted to collect infrared spectra of 35 nm ultrathin films.

2.3. Surface morphology

Atomic force microscopy (AFM) images were recorded at room temperature in air with a NanoScope III multimode AFM (Veeco, Santa Barbara, CA) in standard tapping-mode. Microfabricated silicon tips/cantilevers with a nominal tip radius of curvature of 5–10 nm and spring constant of about 3 N/m were used (Veeco). Topographical and tapping phase contrast images were collected simultaneously by adjusting the free oscillation amplitude (A_0) and the set point tapping mode amplitude (A_{sp}) in order to achieve stable imaging conditions. Image processing was performed by WSxM software [18].

3. Results and discussion

3.1. FT-IR analysis of ultrathin films

PET ultrathin films were analyzed by infrared spectroscopy in transmission mode by taking advantage of the high transparency of the used Si windows in the 4000–1550 cm^{-1} as well as of reasonably limited absorption in the 1550–1000 cm^{-1} region. Typical PET spectra were observed at all investigated thickness as reported in Fig. 2a [19].

The inset of Fig. 2a shows the absorption bands due to the wagging of glycol $-CH_2-CH_2-$ in *gauche* ($\sim$1370 cm^{-1}) and *trans* ($\sim$1340 cm^{-1}) conformation (Fig. 2b), plus the band at 1410 cm^{-1} due to in-plane vibration of the benzene ring [19] frequently used as the normalization band.

PET in the crystalline phase assumes a full *trans* conformation, which means that the glycol segments, the phthalates and the ester moieties are all arranged in *trans* conformation [20,21]. Indeed, the IR conformational bands can be used to follow the PET crystallization process as well as to assess the presence of crystal phase in starting PET films [22]. In particular, the fraction of glycol segment in *trans* conformation (f_T) is carried out as [9,23–25]:

$$f_T = \frac{A_{1340}}{A_{1340} + k \cdot A_{1370}} \quad (1)$$

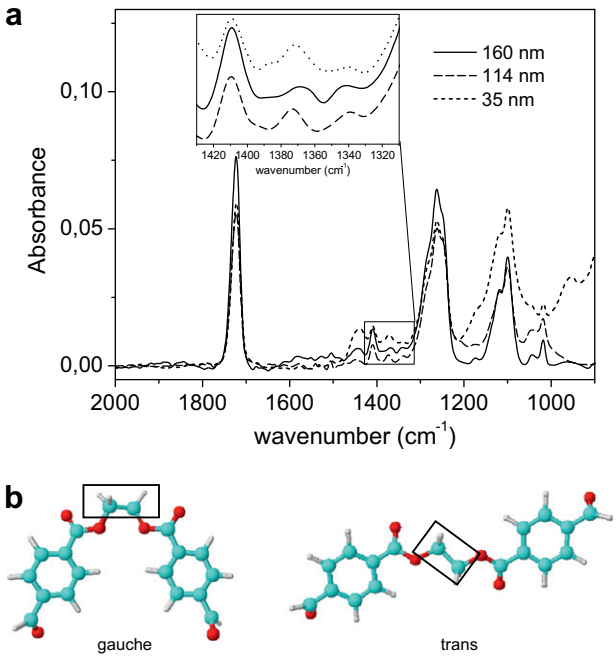

Fig. 2. (a) IR spectra of ultrathin films of PET spin coated on Si windows, (b) Sketch of *trans* and *gauche* conformations of the glycol segment in PET.

In equation (1) A_i are the integrated absorption intensities of the infrared absorption bands having maximum at *i* wavenumber, and *k* is a constant equal to the ratio between the absorption coefficient of the wagging band for the glycol segment in *gauche* and *trans* conformation. The value of *k* was derived for a reference free standing film of PET 20 μm thick [26] to be 6.7, in good agreement with previous used values [9,23,24].

The amount of glycol segments in *trans* conformation in the as-prepared ultrathin films ranged between 0.07 and 0.13, where the lowest amount was found for the 35 nm film. Indeed, it is well known that the glycol segments of PET in the amorphous phase are mostly in the *gauche* conformation, while 10–12% of them are in *trans* conformation [27,28]. That was also our case, and so the absence of relevant amount of crystalline phase in all prepared films was verified.

3.2. Cold crystallization at 107 °C

FT-IR spectra were acquired while ultrathin films of PET were annealed at 107 °C (See Fig. 3 as example). A progressive intensity increase of the band at 1340 cm^{-1}, due to the *trans* glycol conformer, and a corresponding decrease of the band at 1370 cm^{-1}, due to the *gauche* conformer, were observed. This indicates a progressive conversion of *gauche* conformers into *trans* ones, probably due to the cold crystallization process [28].

Other spectral variations over the annealing time were the increase of the bands at 727, 1024, 1110, 1126, 1255, 1271 cm^{-1} and the carbonyl component at 1717 cm^{-1}. Moreover a decrease of the bands at 1093, 1099, 1288, 1240 cm^{-1} and of the carbonyl component at 1732 cm^{-1} were observed. All these spectral variations are typically associated to the formation of crystalline phase [22].

AFM imaging performed both before and after the annealing process showed the presence of crystal and amorphous phases in the samples annealed at 107 °C (see Fig. 4 as an example), while only few or no crystalline seeds are detected in the initial stage images (not reported).

Fig. 4 shows a comparison between surface structures of annealed films of 35 and 160 nm thickness. In both cases, branched spherulite like structures appearing on the surface seem to indicate mainly a flat-on lamellar growth. The crystalline area fraction at the interface with air was obtained from the AFM topography data, by using a threshold procedure already introduced in Ref. [12]:

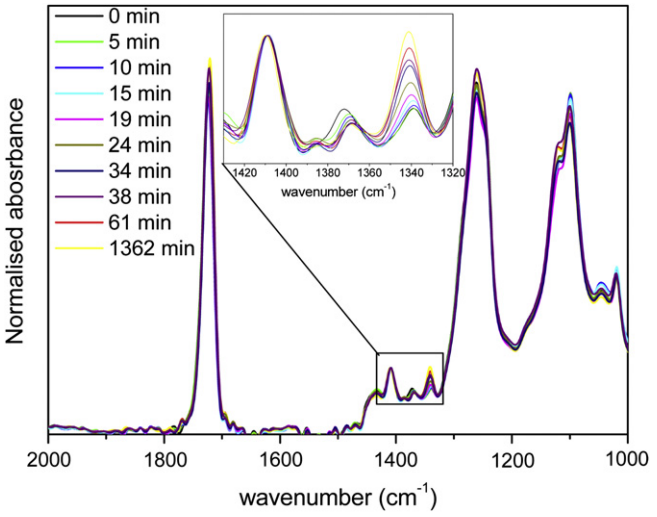

Fig. 3. IR spectra of the 114 nm thin film kept at 107 °C for increasing time (see legend). Spectra were normalized with respect to the maximum intensity of the band at 1410 cm^{-1}.

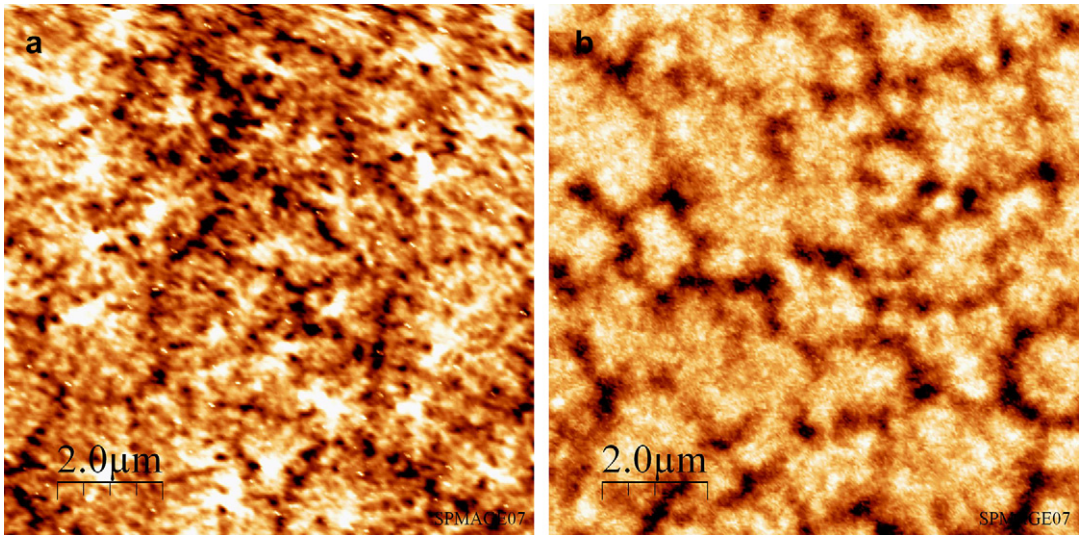

Fig. 4. AFM images of (a) 35 nm and (b) 160 nm films after 1360 min annealing at 107 °C.

a statistical analysis of topographic images estimated a crystalline area fraction of 91 ± 8% and 87 ± 6%, respectively for the film of 35 and 160 nm thickness. This value is much larger than the crystal volume fraction we found by FT-IR on the same PET thin films (see next subsection). Such crystalline fraction is also dramatically larger than the value of 30–35% found by different techniques (XRD, FT-IR, calorimetry, dielectric spectroscopy) on bulk PET samples annealed at the same temperature [26,29–31]. Actually, a very high level of crystal area fraction is a typical feature of the air/polymer free surface and it has been already observed by AFM analysis of several bulk polymeric films [32] included PET [12]. Similarities between the surface crystallization patterns and fraction in films of different thickness could indicate that the substrate and confinement effect are not able to hinder the faster surface crystallization dynamics even in the thinnest films.

3.3. Crystallization and conformation

An usual method to compare the crystal volume fraction in films at different thickness, is to normalize the area value of the *trans* conformer band at 1340 cm^{-1} (A_{1340}) with the reference band area at 1410 cm^{-1} (A_{1410}) [13,19,33] because the latter is assumed to be not affected by conformational change of the monomeric unit. This procedure was attempted to compare the crystallization kinetics in films of different thickness (Fig. 5) but showed a marked discrepancy for the 35 nm film, while a coherent behavior was observed for all the other samples. The values of the area ratio at the end of the observation time, that is in the fully crystallized films, were ~2.2 for the 35 nm film and ~0.9 for all the others. This last value is in agreement with the value observed by N. W Hayes et al. [13] in a 150 nm thick PET film spin-cast on a silicon wafer, analyzed by FT-IR in transmission mode after annealing for 30 min at 110 °C. The high ratio value in the 35 nm film here obtained seems to indicate the formation of a larger final amount of crystalline phase in the thinnest film than in the others. This is the opposite of what was observed for ultrathin PET [9] and poly (ethylene-vinyl acetate) films [15] on gold, where a reduction of both the nucleation rate and the crystalline degree were observed when the film thickness became comparable to the gyration radius of the polymer.

We observed that the A_{1340}/A_{1410} ratio value in the 35 nm film was larger than in all the other films at any annealing time, including the initial time. Such ratio was 1.5 times larger at the beginning, increasing up to 2.5 times at the longest analysis time. The initial content of glycol segments in *trans* conformation (f_T) calculated by using equation (1) and the band intensities in the spectra of the 35 nm film at room temperature indicated instead a lower value in the 35 nm film than in the other films. The dependence of the two band areas on the film thickness was investigated to look into the apparent contradiction. In fact, in

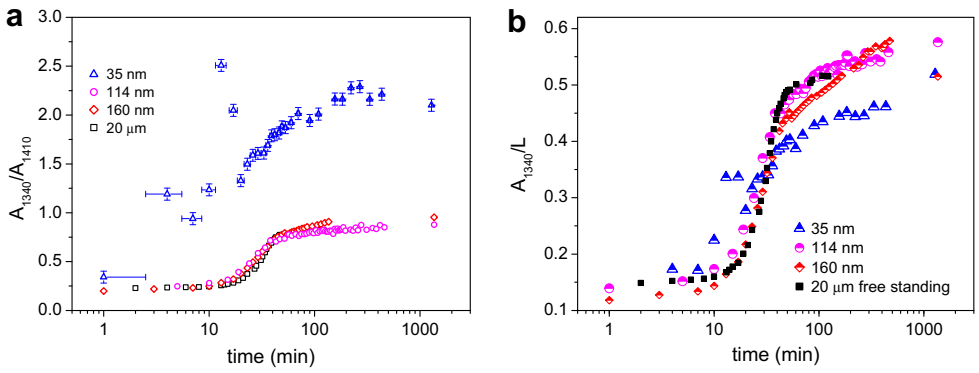

Fig. 5. Normalized area values of the *trans* conformer band (at 1340 cm^{-1}) for PET films on Si windows annealed at 107 °C for different times. Normalization was performed with respect to the reference band at 1410 cm^{-1} (a) or with respect to the film thickness (b).

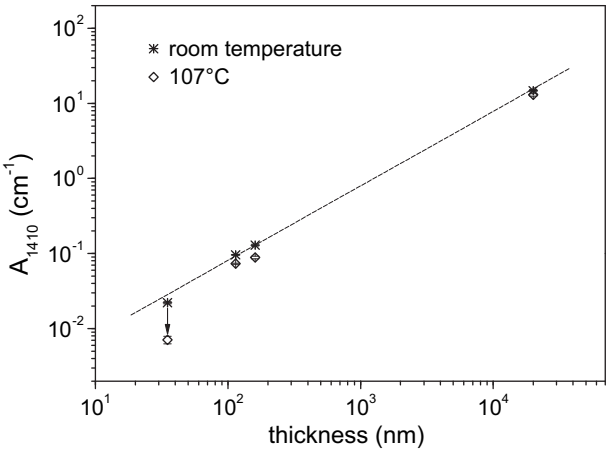

Fig. 6. Area of the band at 1410 cm^{-1} measured in films of different thickness, plotted on double logarithmic scale, in the case of spectra at room temperature and at 107 °C. Values at 107 °C were averaged over the whole annealing time, and the standard deviation was assumed as error (not well evident in the plot because comparable to the symbol dimension). The dashed line represents a linear fit of data at room temperature, with a correlation coefficient of $R^2 = 0.9986$.

transmission mode, with incidence angle of 0° and absorbance values smaller than 0.6–1, the band intensity should be proportional to the film thickness according to the Lambert–Beer law [34]. On the contrary, no linearity was observed for the ring vibration band, as the 35 nm film value at 107 °C was lower than expected (Fig. 6). This deviation must be responsible of the discrepancy in Fig. 5a, and indicates that the band at 1410 cm^{-1} should not be used as reference band. The statement is confirmed by Fig. 5b where comparable plots are observed for the films at different thickness by normalizing the areas of the *trans* conformer band with respect to the film thickness obtained by profilometry measurements (Fig. 5b). A slightly lower crystal content in the 35 nm films than in the thicker films is found, in agreement with the results previously obtained for PET films deposited on gold [9].

In order to analyze the possible source of discrepancy for the intensity of the ring vibrational band at 1410 cm^{-1} in the 35 nm film, a couple of hypotheses can be formulated: (1) at the air interface, intermolecular and intramolecular forces of PET chains are lower than in the bulk, so that the intensity decrease with temperature of the aromatic ring band at 1410 cm^{-1} [35] is larger in the thinnest film, (2) the substrate induces optical anisotropy, visible in the case of the thinnest film, whose infrared spectrum shows a band ratio that differs from that of the corresponding isotropic material [36].

The first hypothesis was stimulated by the observation that the area value of the 1410 cm^{-1} band in the 35 nm film at 107 °C was 68% lower than at room temperature (Fig. 6), not changing appreciably all over the annealing time. The corresponding decrease for the 20 μm film was 12%, in good agreement with previous findings [35], while decrease of 31% and 24% was observed for the 160 and 114 nm films, respectively. The area values at room temperature varied quite linearly with film thickness (Fig. 6). A small deviation from the linear model was observed for the thinnest film, whose area was lower than predicted. The discrepancy at 107 °C was much larger than at room temperature. Based on Ref. [35], such intensity decrease observed at 107 °C with respect to room temperature in PET films on silicon would be expected at temperature higher than 200 °C. In Ref. [35] the effect of temperature on the intensity of the *trans* conformer band at 1340 cm^{-1} was also analyzed, and a larger effect than for the above mentioned ring vibration band was observed. Therefore, under the hypothesis of a less dense packaging in the 35 nm film than in the thicker films, the A_{1340}/A_{1410} band ratio would be expected to be lower for the 35 nm film than for the others. On the contrary it was higher (Fig. 5a). However, the above mentioned analysis of the temperature effect in the *trans* conformer band intensity was performed in a fully crystallized film, to avoid the concurrence of conformational change effects. Therefore the observed behavior is relative to the crystal phase, so that a smaller decrease of the *trans* band intensity with temperature in the amorphous phase cannot be excluded.

The second hypothesis on the cause of the low intensity of the 1410 cm^{-1} band at 107 °C was stimulated by recent papers concerning the dichroic character of the 1410 cm^{-1} band [37,38]. Indeed, in IR spectroscopy, the component of the dipole moment in the wave propagation direction does not contribute to the absorption intensity. Unfortunately no information on the orientation of the transition moment related to the vibration mode responsible of the band at 1410 cm^{-1} is available in literature. However, the band at 1410 cm^{-1} is widely accepted as reference band to follow the *gauche* to *trans* conformational conversion, particularly in oriented films under stress in the plane normal to the propagation vector [28,39,40]. In any case, by considering that the vibration is in-plane, the corresponding vector should lie in the aromatic ring plane. Therefore the low intensity of the 1410 cm^{-1} band in the 35 nm film could be due to an excess of aromatic rings oriented perpendicular to the Silicon surface than in the isotropic PET material. In Fig. 7 the

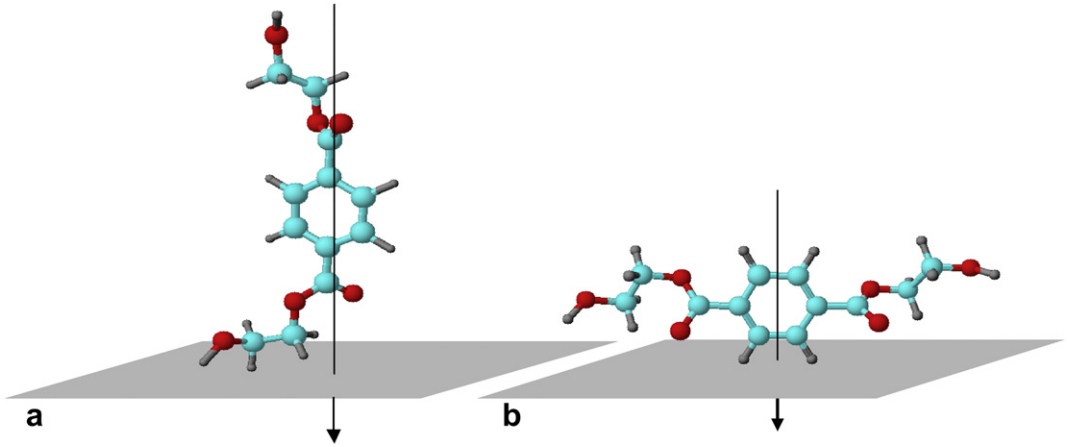

Fig. 7. Possible arrangements of the aromatic ring of PET unit perpendicular to a surface.

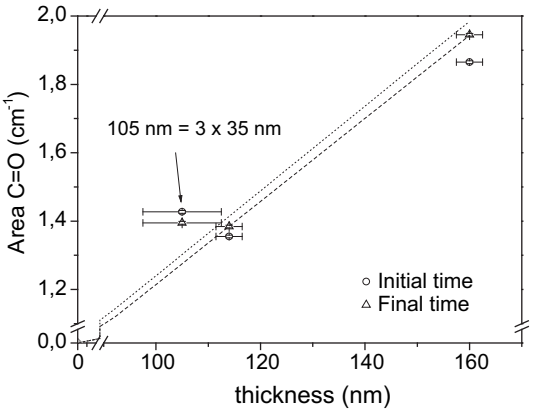

Fig. 8. Area of the carbonyl stretching band at ~1720 cm^{-1} in the FT-IR spectra of films with different thickness.

two possible orientations of the aromatic ring perpendicular to the silicon surface are illustrated.

Furthermore, the carbonyl stretching band at ~1720 cm^{-1} on the 35 nm film was observed to have higher intensity than expected for such film thickness (Fig. 8). The carbonyl group is oriented mostly perpendicularly to the PET chain axis. The vibration dipole moment has the same orientation of the group itself, therefore the observed very high level of intensity could be due the orientation of macromolecular chains perpendicular to the Si surface, as sketched in Fig. 7a.

The perturbation responsible for such orientation can be caused by the confinement effect or by the presence of the Silicon substrate. The effect of the interface with air can instead be excluded, since it should favor parallel orientation of the benzene ring [41]. As mentioned before, the A_{1340}/A_{1410} band ratio in the 35 nm film, at the initial stage, was 1.5 times higher than for the other films, and became 2.5 times higher after annealing at 107 °C. Such increase of discrepancy seems to indicate that the initial orientation also promotes orientation of the crystal phase, with lamellae parallel to the silicon interface (flat-on lamella growth), as also confirmed by AFM images.

On the other hand, since the *trans* conformer wagging band vector forms an angle of 21° with the macromolecular chain axis [42,43] the corresponding band intensity should be decreased by the perpendicular orientation with respect to the silicon surface. Therefore, the low intensity of the *trans* conformer band in the 35 nm film with respect to the others (Fig. 5b) at the end of the crystallization time does not necessarily indicate a lower crystal content in the 35 nm film but could be due only to an orientation effect.

Unfortunately, for the 35 nm film, the *gauche* conformer band intensity decreased beyond the minimum detectable value as soon as annealing started. Therefore, the procedure based on fraction of *gauche* and *trans* conformers (equation (1)) could not be applied to calculate the crystalline fraction over the annealing time, but it could only be used to determine the starting *trans*/*gauche* ratio.

Several routine methods such as DSC, XRD and density measurements are available to confirm IR spectroscopy indications for thick films, but these methods cannot be used for ultrathin films.

To confirm that the correspondence between conformational change and crystallization during annealing is also valid in thin films, evaluation of the infrared band positions in a comparative way in thin and thick films was performed. Indeed, accordingly to the results by Cole et al. [22] the wavenumber of the maximum of the *trans* conformer band is associated to the crystalline fraction. Two positions for the maxima of the *trans* conformer bands in infrared spectra are identified, one at 1343.0 cm^{-1} for the crystalline ordered phase, and the second one at 1339.5 cm^{-1} for the glycol segments in *trans* conformation in a disordered amorphous phase. Films with a mixture of the two phases exhibit intermediate band position resulting by the overlap of the two components. Consistently, initial band maxima in the free standing reference thick films, which showed no detectable crystallinity by XRD and DSC analysis, was located at 1339.8 cm^{-1} (Fig. 9a). The band maximum shifts toward higher wave-numbers while the film is annealed at 107 °C. A plot of this quantity versus time displays a sigmoid shape with inflection at 1341.3 cm^{-1} and plateau at 1341.8 cm^{-1}. The final value was lower than the value of 1343 cm^{-1} indicated in Ref. [22] for the completely ordered phase. Thus, a lower degree of order is indicated, in accordance with the general finding for PET crystals grown in the 100–120 °C temperature range [34,44].

The kinetic behavior of the reference sample can be compared to that of thin films. Before annealing, band maxima are located at lower wavenumber than in the reference film. Moreover, the band maxima further decreased at the beginning of the annealing stage (Fig. 9a), to increase again similarly to what observed in the free standing film. The red shift with respect to the free standing film persisted all over the observation time. If the band shift ($\nu-\nu_0$) vs. time is normalized with respect to the maximum observed shift ($\nu_{inf}-\nu_0$), similar sigmoidal graphs are obtained (Fig. 9b). Therefore the two graphs are just shifted to one another and the observed band intensity increases while annealing can be associated to the formation of similar crystalline phase in the thin and thick films. Moreover, the analysis of the inflection points showed faster

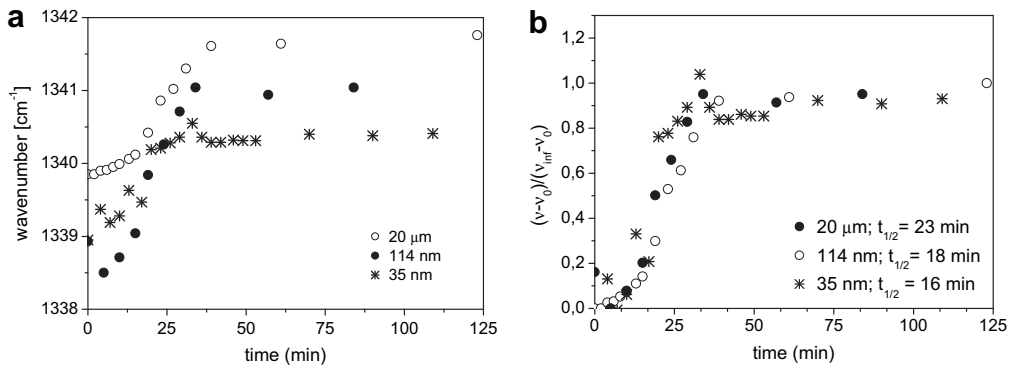

Fig. 9. Wavenumber of the *trans* conformer band at maxima (a) and corresponding reduced frequency shift (b) (see text). Results for 160 nm thin film are not reported since in such case spectral data were not suitable for application of band shift method, due to insufficient spectral resolution.

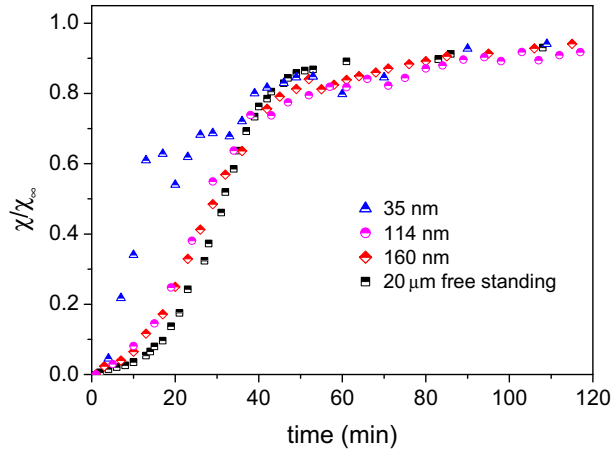

Fig. 10. Plots of the relative crystallinity growth over time in a thick free standing film and in ultrathin PET films on Si.

kinetics with thickness decrease (Fig. 9b), as also observed in the comparison of Fig. 5b.

The systematic band maxima shift toward the red in the thinnest films with respect to the reference may indicate a less dense packaging of PET chain similar to the temperature effect reported in Ref. [35], as suggested also by the observed low intensity of the aromatic ring vibration band.

3.4. Avrami analysis

The comparison in Fig. 5b shows that the variation of the intensity of the *trans* conformer band is a little bit faster in the ultrathin films than on the free standing film. Such difference is more evident for the thinnest film, namely the 35 nm one. In order to investigate more deeply the mentioned differences, the variation of the amount of crystal phase during the annealing time at 107 °C was compared for ultrathin and thick films. If the amount of glycol in *trans* conformation (f_T) was assumed as linearly varying as the crystal phase volume fraction [20,21] then the relative amount of crystal phase at time t, that is, χ/χ_∞, could be calculated as:

$$\frac{\chi}{\chi_\infty} = \frac{f_T - f_{T0}}{f_{T\infty} - f_{T0}} \tag{2}$$

the subscript 0 and ∞ refer to the f_T value at time zero and at equilibrium, respectively. In the case of the 35 nm film, as already mentioned, the signal to noise ratio for the *gauche* conformer band was too low, so the unnormalized *trans* area band was used in such case instead of the f_T value. The obtained plots are compared in Fig. 10, where differences among the crystallization kinetics for films of different thickness are evident.

The growth of crystal phase (α) over time under isothermal conditions is usually described in terms of the semiempirical Avrami's model

$$\alpha(t) = 1 - \exp(-Kt^n) \tag{3}$$

where α is the crystalline fraction, K is a constant which can be expressed in terms of the characteristic time of the process τ_c as $K = 1/\tau_c$, and n is a parameter whose value depends on the occurrence of nucleation [45] and on the dimensionality of the growth process. For a semicrystalline solid, $\alpha(t)$ is given by the relative amount of crystal phase at time t, that is χ/χ_∞. According to the most of the polymer crystallization models [2], the parameter n assumes the value of 4 for the spherical crystallization under fast radial growth with thermal nucleation in a large sample, where the effect of the interface can be neglected. On the contrary, the value of n can be smaller than 4 because of many effects: very fast nucleation (for instance heterogeneous nucleation by impurities, nucleants or interfaces), slow radial growth, orientation and confinement effects [46,47]. The radial growth rate and the nucleation rate in isotropic pure polymers depend mostly on the attitude of the polymer to crystallize, as well as on the temperature of crystallization; therefore such rate can be assumed to be constant for a given polymer which crystallizes isothermally. In order to find the reference value of n for the PET used in the present study undergoing isothermal crystallization at 107 °C, the value for the reference thick film was estimated as follows. We adopted a standard method consisting in the linearization of the Avrami's equation (3), by plotting data in bilogarithmic scale (Fig. 11) [2]. The resulting graph in the case of equation (3) is a straight line with slope n and intercept $-\ln K$. However, as commonly observed in literature for the crystallization of polymers [21,48], a deviation from the straight behavior at short times is observed for our data. Such deviation is often ascribed to the presence of a delayed start of the crystallization, named induction time (t_0). This delay can be connected to the time required to establish thermal equilibrium in the sample, or for the polymer chains to relax and allow the formation of the first crystal nuclei. The deviation was observed for all studied films, included the thick one (Fig. 11a). Actually a simple temperature delay is not likely for timescale of several minutes, due to the fast equilibration time of our apparatus and the small mass involved by the system sample/Si window.

Fitting of the linear part of the plot with a straight line provides the values of n and $-\ln K$ shown in Table 1. The reference film (thick

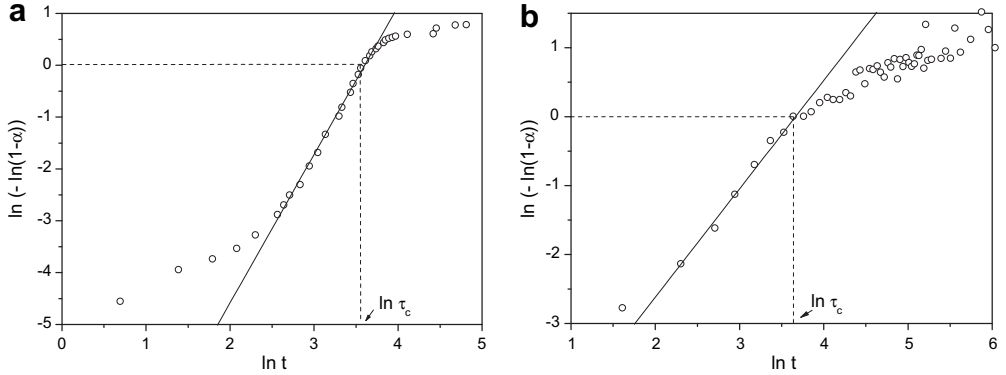

Fig. 11. Comparison between the Avrami's plots for PET crystallization in a thick free standing film (a) and in the 114 nm film on Si (b).

Table 1
Crystallization parameters obtained by data analysis with Avrami and Avramov methods.

Thickness (nm)	$t_{1/2}$ (min)	τ_c (min)	n	ln K	t_0 (min)	τ_1 (min)	n
			Avrami			*Avramov*	
20 000	32	36	2.9	10.3	21	11	2.9
160	29	36	2.1	7.5	12	17	1.9
114	29	36	2.1	7.5	15	14	1.7
35	15	26	0.9	2.9	0	10	0.9

free standing) shows a characteristic time τ_c of the process of 36 min under the conditions of our study. Such time is slightly longer than the crystallization half time $t_{1/2}$ (also reported in Table 1) defined as the time at the inflection point of the sigmoid plot of Fig. 9 (32 min). The latter is in agreement with the value of 33 min from DSC analysis reported in Ref. [31] for the isothermal crystallization of PET at a similar temperature. Moreover, the same sample was analyzed by DSC, XRD, and dielectric spectroscopy (DS) [26] and the results confirmed the value of 32 min here obtained by FT-IR analysis. τ_c can be expressed as the sum of the induction time (t_0) and a characteristic time τ_1 that better describes the system kinetics. Such time is derived from the intercept of the x axis by the function $\ln(-\ln(\chi/\chi_\infty))$. The value of n found for the reference film was 2.9 which is quite typical for films of polyesters that crystallize slowly, particularly under cold crystallization conditions [49–51]. In Ref. [47] it is shown that the Avrami's exponent can be as small as 2.2 in 50 μm films, when the potential nuclei number is low, as well as the activation rate.

The comparison of the induction time in the reference free standing film and ultrathin films can also provide useful information on thickness dependence of crystallization. Experimental data were therefore analyzed by the method proposed by Avramov et al. [48], which allows the evaluation of the induction time t_0. Moreover, the Avramov's method has the advantage that the derived characteristic time of the process is scarcely affected by the scattering of data at the beginning and at the end of the observation time. This aspect can be important for the case here analyzed, where some unclear phenomena are present during the induction time. In the Avramov's method, the relative crystallinity (χ/χ_∞) is plotted versus the natural logarithm of time (Fig. 12a). The χ/χ_∞ derivative plot is calculated, so that its maximum provides $\tau_1 + t_0$ where τ_1 is the true characteristic time of the crystallization process and t_0 the induction time. Avramov proved that such maximum should be at $\chi/\chi_\infty = 0.63$ when the induction time is zero. Therefore, t_0 is the time at which the χ/χ_∞ versus ln $(t-t_0)$ has its maximum at $\chi/\chi_\infty = 0.63$ (Fig. 12). By this method, an induction time of 21 min was obtained for the free standing film. The Avramov method allows also to obtain the n parameter from the slope b at the inflection point of the bilogarithmic plot, by evaluating $n = e\ b$. The value found for the reference film is 2.9, in good agreement with the value found with the classical Avrami's method.

The Avrami and Avramov methods were both applied to obtain the n parameters for all the thin films on Silicon. The values obtained by the two methods are in good agreement between them by taking into account the data scattering, particularly in the Avrami method (Table 1). The n values for the ultrathin films decrease with the film thickness. Similar behavior was observed also by Zhang [9] who found values from 2.3 to 1.2 for PET films on gold with thickness from 115 to 22 nm crystallized at 105 or at 110 °C. On the other hand, in spite of the similar decrease of the exponent, the crystallization half time $t_{1/2}$ on gold was found to increase with the film thickness, that is the opposite to what was here observed on Si (Table 1).

The decrease of the n exponent in confined environment has been the subject of many theoretical works which interpreted the experimental evidences showing a decreasing crystallization rate in thin films because of the lower probability of polymer volume located near the interface to be included in spherulites with respect to bulk volume [16]. The cited approach predicts a decreasing crystal amount and rate with film thickness decrease, as found for the gold substrate. On the contrary, we observed an increasing crystallization rate with thickness decrease and comparable crystal amount at least in films 20 μm, 160 nm and 114 nm thick. This experimental observation strongly indicated that our results cannot be explained only by geometrical considerations. Indeed, the infrared band maxima position indicated an higher order degree around the trans glycol unit in the thinnest film than in the others and the *trans* glycol segments initially in the film are those that may evolve into potential crystal nuclei. Moreover we can also infer a preferential orientation of chains close to the substrate in the thinnest film that was not observable in the thicker samples.

The half time of the crystallization process ($t_{1/2}$) (Table 1) was scarcely affected by the thickness decrease, except for the thinnest film of 35 nm. This difference was evidenced also by the characteristic time of the process τ_1, as obtained by the Avramov method. Because of the data scattering especially at the beginning of the observation time, there is quite a large difference between the $t_{1/2}$ and the τ_c values. In that case, the Avramov method allows to overcome the drawback of data scattering and provides a characteristic time of the process τ_1 of 10 min for the 35 nm film, which, due to data scattering, seems to be comparable to the corresponding values in the films with higher thickness. Moreover, the Avramov method

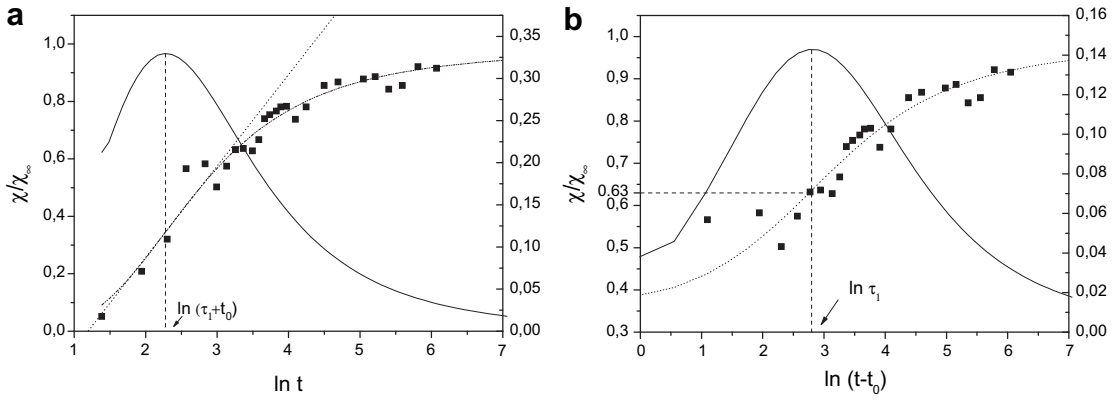

Fig. 12. Avramov's plots for PET crystallization in a 35 nm film on Si. Plot in ln t (a) and ln $(t-t_0)$ (b). Solid lines represent the derivative plots.

allows to evidence a decrease of the induction time t_0 with the film thickness decrease which most likely can be connected to the rate of activation of the potential nuclei due to a higher mobility of chains in the 35 nm film than in the thicker ones.

The most part of literature data related to crystallization in thin and ultrathin polymeric films shows a decrease of crystal amount and crystallization rate with thickness decrease [9,15]. Here we report an experimental evidence of increasing crystallization rate with film thickness decrease. This behavior was predicted by Reiter and coworkers for crystallization in films on slippery walls [17]. The surface energy of amorphous silicon is 1.05 J/m^2 [52], lower than the corresponding values of materials typically used as polymer substrates, like gold, aluminium, and silicon oxide [53]. Moreover, when the film thickness decreases to few nanometers, not only the substrate interface but also the air interface becomes important to the overall dynamic behavior. Indeed, the crystallization of PET at the air interface has been found to be faster than in the bulk [11] and thus most likely the observed increased crystallization rate as the film thickness decrease could be due to the predominant effect of the interface with air over that with the amorphous silicon substrate.

4. Conclusion

Infrared spectroscopy was employed to follow the formation kinetics of crystal phase in PET 160, 114 and 35 nm thin films spin-coated on amorphous silicon and annealed at 107 °C. Crystallization kinetics was found slightly faster in the thinnest film with a decrease of both the Avrami exponent and the induction time of the crystallization. The effect becomes larger with the film thickness decrease. Occurrence of surface crystallization was confirmed by AFM morphology analysis.

An unexpected low intensity of the ring vibration IR band at 1410 cm^{-1} was observed at 107 °C, which can be interpreted as orientation effect of the PET chains perpendicularly to the silicon substrate or in terms of a low density packaging of PET chains in the ultrathin films, particularly evident in the case of the 35 nm PET film.

All such phenomenology suggests a trend that is at odds with respect to previous observation on PET ultrathin films. We attributed it to the dominant effect of the air interface over the scarcely interacting silicon surface: the overall result is to make the PET chains more mobile and prompt to order and nucleate.

Acknowledgements

We thank P. Stagnaro (ISMAC Genova) for SEC analysis, D.Prevosto, M. Lucchesi, P.A. Rolla and F. Ciardelli for stimulating discussion, and M. Bianucci for technical support.

References

[1] Alcoutlabi M, McKenna GB. J Phys Condens Matter 2005;17:R461–524.
[2] Wunderlich B. Crystal nucleation, growth, annealing. In: Macromolecular physics, vol. 2. New York: Academic Press; 1976.
[3] Basset DC. Principles of polymer morphology. New York: Cambridge University Press; 1976.
[4] Piorkowska E, Galeski A, Haudin JM. Prog Polym Sci 2006;31:549–75.
[5] Hobbs JK, Farrance OE, Kailas L. Polymer 2009;50:4281–92.
[6] Hu W, Cai T, Ma Y, Hobbs JK, Farrance O, Reiter G. Faraday Discuss 2009;43:129–41.
[7] Zhang Y, Zhang J, Lu Y, Duan Y, Yan S, Shen D. Macromolecules 2004; 37:2532–7.
[8] Napolitano S, Prevosto D, Lucchesi M, Pingue P, D'Acunto M, Rolla P. Langmuir 2007;23:2103–9.
[9] Zhang Y, Lu Y, Duan Y, Zhang J, Yan S, Shen D. J Polym Sci Polym Phys 2004; 42:4440–7.
[10] Orench IP, Stribeck N, Ania F, Baer E, Hiltner A, Calleja FJB. Polymer 2009; 50:2680–7.
[11] Jukes PC, Das A, Durell M, Trolley D, Higgins AM, Geoghegan M, et al. Macromolecules 2005;38:2315–20.
[12] De Cupere VM, Rouxhet PG. Polymer 2002;43:5571–6.
[13] Hayes NW, Beamson G, Clark DT, Law DSL, Raval R. Surf Interface Anal 1996;24(10):723–8.
[14] Schönherr H, Frank CW. Macromolecules 2003;36:1188–98.
[15] Elzein T, Brogly M, Schultz J. Surf Interface Anal 2003;35:785–92.
[16] Billon N, Haudin JM. Colloid Polym Sci 1889;267:668–80.
[17] Ma Y, Hu W, Reiter G. Macromolecules 2006;39:5159–64.
[18] Horcas I, Fernández R, Gómez-Rodríguez JM, Colchero J, Gomez-Herrero J, Baró AM. Rev Sci Instrum 2007;78:013705.
[19] Boerio FJ, Bahl SK, McGraw GE. J Polym Sci Polym Phys 1976;14:1029–48.
[20] Fina LJ, Koenig JL. Macromolecules 1984;17:2572–9.
[21] Jog JP. Polym Rev 1995;35(3):531–53.
[22] Cole KC, Ajji A, Pellerin E. Macromolecules 2002;5:770–84.
[23] Wang Y, Shen DY, Qian RY. J Polym Sci Polym Phys 1998;36(5):783–8.
[24] Qian RY, Shen DY, Sun FG, Wu LH. Macromol Chem Phys 1996;197 (4):1485–93.
[25] Matsuo M, Luo YL, Galeski A. Phys Rev E 2009;79(4):041801.
[26] Bertoldo M, Capaccioli S, et al. unpublished results.
[27] Stokr J, Schneider B, Doskocilova D, Lovy J, Sedlacek P. Polymer 1982;23 (5):714–21.
[28] Kirov KR, Assender HE. Macromolecules 2005;38:9258–65.
[29] Alvarez C, Sics I, Nogales A, Denchev Z, Funari SS, Ezquerra TA. Polymer 2004;45:3953–9.
[30] Ezquerra TA, Sics I, Nogales A, Denchev Z, Baltà-Calleja F. JEPL 2002;59 (3):417–22.
[31] Aref-Azar A, Arnoux F, Biddlestone F, Hay JN. Thermochim Acta 1996;273:217–29.
[32] Kortaberria G, Marieta C, Jimeno A, Arruti P, Mondragon I. J Microsc 2006;224 (3):277–89.
[33] Richards PD, Weitz E, Ouderkirk AJ, Dunn DS. J Phys Chem 1993;97:12061–6.
[34] Tolstoy VP, Chernyshova IV, Skryshevsky VA. Handbook of infrared spectroscopy of ultrathin films. New York: Willey-Intersience; 2003.
[35] Lin SB, Koenig JL. J Polym Sci Polym Phys 1983;21:2067–83.
[36] Bungay C, Tiwald TE. Thin Solid Films 2004;455:272–7.
[37] Pellerin C, Pezolet M, Griffiths PR. Macromolecules 2006;39:6546–51.
[38] Laskarakis A, Logothetidis S. J Appl Phys 2007;101(5):053503.
[39] Guhremont J, Ajji A, Cole KC, Dumoulin MM. Polymer 1995;36(17):3385–92.
[40] Everall NJ, Chalmers JM, Local A, Allen S. Vib Spectrosc 1996;10:253–9.
[41] Durell M, Macdonald JE, Trolley D, Wehrum A, Jukes PC, Jones RAL, et al. Europhys Lett 2002;58(6):844–50.
[42] Walls D. J Appl Spectrosc 1991;45(7):1193–8.
[43] Spiby P, O'Neill MA, Duckett RA, Ward IM. Polymer 1992;33(21):4479–85.
[44] Kong Y, Hay JN. Eur Polym J 2003;39:1721–7.
[45] Wunderlich B. In: Turi EA, editor. Thermal characterization of polymeric materials, vols. 1 and 2. San Diego: Accademic Press; 1997.
[46] Cheng SZD, Wunderlich B. Macromolecules 1988;21(11):3327–8.
[47] Escleine JM, Monasse B, Wey E, Haudin JM. Colloid Polym Sci 1984;262 (5):366–73.
[48] Avramov I, Avramova K, Russel C. J Cryst Growth 2005;285:394–9.
[49] Lu X, Hay JN. Polymer 2000;41:7427–36.
[50] Slobodian P. J Therm Anal Calorim 2008;94(2):545–51.
[51] Napolitano S, Wübbenhorst M. J Non-Cryst Solids 2007;353:4357–61.
[52] Hara S, Izumi S, Kumagai T, Sakai S. Surf Sci 2005;585:17–24.
[53] Pieruccini M, Flores A, Nochel U, Di Marco G, Stribeck N, Calleja FJB. Eur Phys J E 2008;27:365–73.